Geologie en Mijnbouw **71**: 71–80, 1992.

Unravelling the progressive strain-history of rocks in metamorphic areas, the example of the Somero area, SW Finland

Robert J. Konert, Harm Stel & Paul H.M. Reemst
Institute of Earth Sciences, Vrije Universiteit Amsterdam, De Boelelaan 1085, NL-1081 HV Amsterdam, the Netherlands

Received 3 June 1991; accepted in revised form 21 January 1992

Key words: deformation, dome structures, strain analyses, structural elements

Abstract

The progressive three-dimensional strain path of rocks during their metamorphic evolution and the relation between strain and structural elements were studied in the Somero area, SW Finland. All the methods used involve two basic steps: determination of two-dimensional strain ellipses on several planes and subsequent calculation of three-dimensional strain ellipsoids from the two-dimensional strain ellipses. Strain analyses were performed on: (1) deformed objects in agglomerates and xenoliths, providing finite strain values and (2) the spatial distribution pattern of cordierite and garnet porphyroblasts, reflecting F_2 and F_3-strain. The two types of strain markers have not been found together in one exposure. A test of the spatial distribution pattern method in terms of shape and orientation has been applied to cordierite porphoryblasts. These blasts show deformation substructures indicative of dislocation creep and have ellipsoidal shapes. Their shapes correlate closely with the results of the spatial distribution pattern method. The methods provide the possibility of obtaining strain data in metamorphic areas.

Introduction

One of the main problems in unravelling the tectonic history of high-grade fold-belts is to decipher the progressive strain path during the metamorphic evolution. This paper deals with such a problem in the Svecofennian Gneiss and Schist Belt, SW Finland. Strain analyses were performed on deformed objects in agglomerates and xenoliths and on the spatial distribution pattern of porphyroblasts. We investigate whether the combination of these methods yields additional information both on the progressive strain path of rocks and the relation between successive structural elements with strain data.

The Somero area is situated in the Svecofennian Belt. The belt is characterised by supracrustal rocks, intruded by syn- to pre-tectonic granitoids. Supracrustals are predominantly metavolcanics, i.e. agglomerates, felsic and mafic tuffs and pillow amphibolites with intercalations of (mica) schists and minute amounts of quartzites and marbles. Infracrustals are mainly migmatites and granitoids, i.e. microcline granites, granodiorites, tonalites and gabbros.

Hietanen (1975) interpreted the Svecofennian metamorphic terrain as an ancient island-arc environment. Zircon cyrstals of the synorogenic plutonic and metavolcanic rocks yield ages between 1920 and 1880 Ma (Simonen 1980). At 1700–1550 Ma ago, the rock succession was locally intruded by Rapakivi granites, e.g. the Laitila and Vehmaa massifs (Windley 1986).

The infra- and supracrustal rocks of this Sveco-

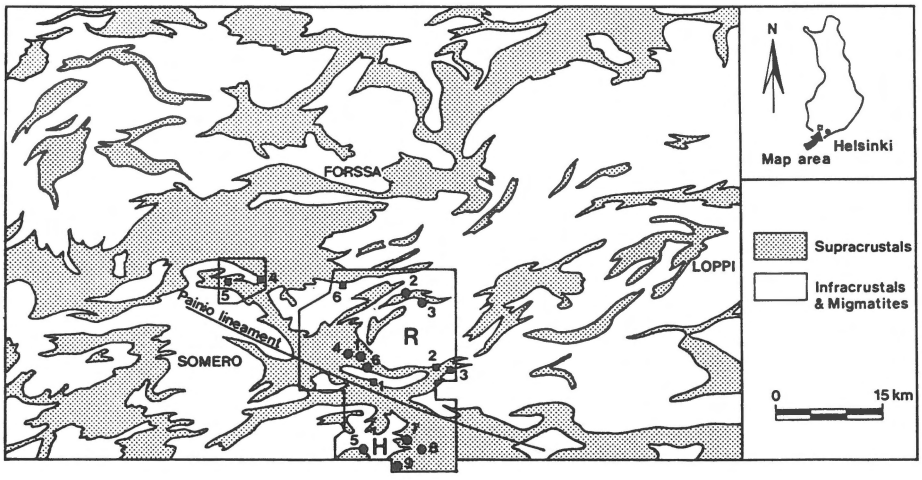

Fig. 1. Simplified geological map of SW Finland; modified after Griffin (1979). Sample locations are superimposed with dots for cordierite and garnet porphyroblast distributions, and with squares for agglomerates and xenoliths. R = Ruostejärvi dome and H = Halkjärvi dome. Location numbers correspond with those in Figs. 5 and 7. Detail map outlines refer to Fig. 8.

fennian Belt have been metamorphosed under low-pressure amphibolite to granulite facies conditions (Dietvorst 1981, Schreurs 1985). The relation between the deformation phases and metamorphic minerals is shown in Table 1.

In the metapelitic rocks, three fold generations have been developed by polyphase deformation. The first phase of deformation (F_1) formed a regional foliation (S_1) and is the axial plane foliation of isoclinal, intrafolial folds. S_1 displays a well developed differentiated layering. During a second phase of deformation (F_2) open to isoclinal folds have been formed. The crenulation cleavage S_2 has been generated as the axial plane foliation of F_2-folds. F_3-structures are characterised by antiformal, dome-like structures. Major approximately WNW and NNE striking subvertical F_4-shear zones have been recognised throughout the entire belt.

Table 1. Petrogenetic diagram

	F_1	F_2	F_3	F_4
Quartz	———	———	———	———
Plagioclase	———	———	———	———
Biotite	———	———	———	———
White mica	–	———	———	———
Hornblende	——— – –			
Cummingtonite	——— – –			
Diopside	——— – –			
Andalusite	– ——— –			
Sillimanite	– ——— –			
Cordierite	– ——— – – –			
Garnet	– ——— – –			
Pegmatite	———	———	———	——— – – – –
Granite	– – – – – –	———	——— – –	
Migmatite		———	——— –	
Prehnite				– ——— –

The structure of the belt is dominated by the occurrence of kilometre-scale oval-shaped F_3-granite domes (Fig. 1). In the Somero area, two such granite domes with distinct metamorphic evolution and structural style have been recognised (Stel et al. 1989). The first has (sub-) vertical structural elements and consists of granites and migmatites derived from in-situ melting at a relatively early stage of the deformational history. The second is a gently westward plunging antiform with gently to steeply dipping limbs, displaying injection-type migmatisation at a later stage. The two domal structures are interpreted as representing different levels of diapirical structures. In the present paper, we analyse the progressive strain path for the two neighboring dome structures, by comparing finite strain – as recorded by deformed objects – with strain recorded by successive porphyroblast stages.

The strain markers used are different in age, thus allowing the establishment of a strain-history. The strain ellipsoids determined from agglomerates and xenoliths reflect finite strain, while strain ellipsoids derived from cordierite and garnet porphyroblast distributions record F_2 and F_3-strain. Agglomerates and xenoliths do not contain suitable porphyroblasts, which means that the different strain markers have not been found together in one exposure.

This paper sets out to argue that the use of strain markers of a different age is consistent with the detailed structure.

Methods used for strain analyses

Several methods of strain analysis, outlined below, were used, the choice of the method being dependent on the nature of the deformed object. All methods involve two basic steps: first, the establishment of two-dimensional (2D) strain ellipses on several planes and second, the calculation of three-dimensional (3D) strain ellipsoids from the two-dimensional strain ellipses.

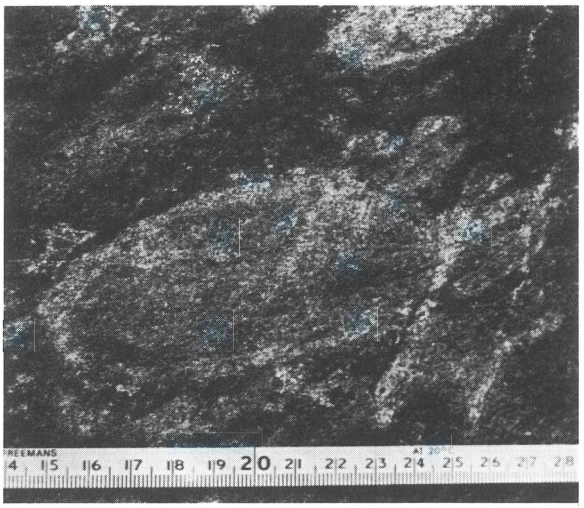

Fig. 2. Outcrop view of deformed bomb-like fragments, location 6720.70–2483.30. Scale bar in cm.

2D strain measurements

The harmonic mean (Spiegel 1972) was used to calculate two-dimensional strain values in rocks containing deformed objects. The harmonic mean is defined as $H = n/(\sum 1/R_d)$, where n = amount of measurements and R_d = axial ratio of deformed object, defined by longest/shortest axis.

Finite strain measurements were performed on agglomerates and xenoliths, having an assumed initial elliptical shape. Lengths of the longest and shortest axes of the bomb-like objects in agglomerates and xenoliths have been measured ($n \approx 20$). Subsequently the harmonic mean was calculated on several planes in an exposure. Next the pitch of the longest axis in relation to the orientation of the dipvector of the exposure plane was determined clockwise using a stereographic Schmidt net.

Fry's method (Fry 1979, Hanna & Fry 1979) is based on the spatial distribution of markers with an initial anti-clustered distribution. The method is based on the interdependence of distance of adjacent porphyroblasts and orientation with respect to the axes of strain. The strain increment after a specific phase of porphyroblastesis was established by this spatial distribution pattern method on cordierite and garnet porphyroblasts, applied to three orthogonal sawing planes.

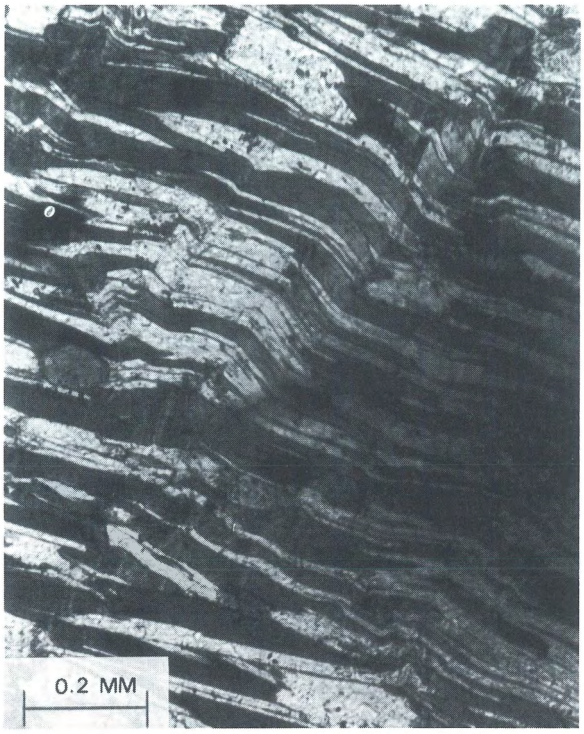

Fig. 3. Optical micrograph displaying detail of F_3-folded S_2.

Fig. 4. Photograph of handspecimen showing cordierite porphyroblast ellipses. Scale indicator in cm.

3D strain calculations

The calculation of the 3D strain was performed by appling Owens' method (Owens 1984) to the 2D strain values. This method determines a best-fitting ellipsoid from three to fifteen sections. In essence, the method formulates a relation between the two-dimensionally measured ellipse in sections and the required three-dimensional ellipsoid. The relationship between the known and unknown factors yields a number of equations, which are solved by means of the least-square treatment (Van Balen & Van Wees 1987).

Sample descriptions

Two rock types were used to determine strain by object-analysis: agglomerates and xenolith-rich metatonalites.

Agglomerates consist of felsic bomb-like fragments (Fig. 2) in a mafic matrix which is rich in clinopyroxene and amphibole. The mineral paragenesis is plagioclase, diopside, hornblende, quartz, titanite and opaques. Xenoliths consist of hornblende-gneiss fragments and occur in metatonalites. The mineral paragenesis is plagioclase and quartz and minor amounts of K-feldspar, biotite and hornblende. A distinct lineation is defined by the preferred orientation of amphibole grains, both in the deformed objects and matrix.

The samples used for analysis with Fry's method are cordierite-mica schists and gneisses and garnet gneisses. The samples are only appropriate when they contain an anti-clustering porphyroblast distribution. The cordierite-mica schists and gneisses have a well developed foliation (S_1 and S_2), defined by seams of brown biotite alternating with quartz-feldspar layers. S_2 shows folding on a microscopic scale (Fig. 3). The mineral paragenesis is quartz, biotite, white mica, plagioclase, andalusite, sillimanite, opaque, tourmaline and cordierite. Locally, both cordierite and garnet occur in a single specimen. Optical and electron microscopical ob-

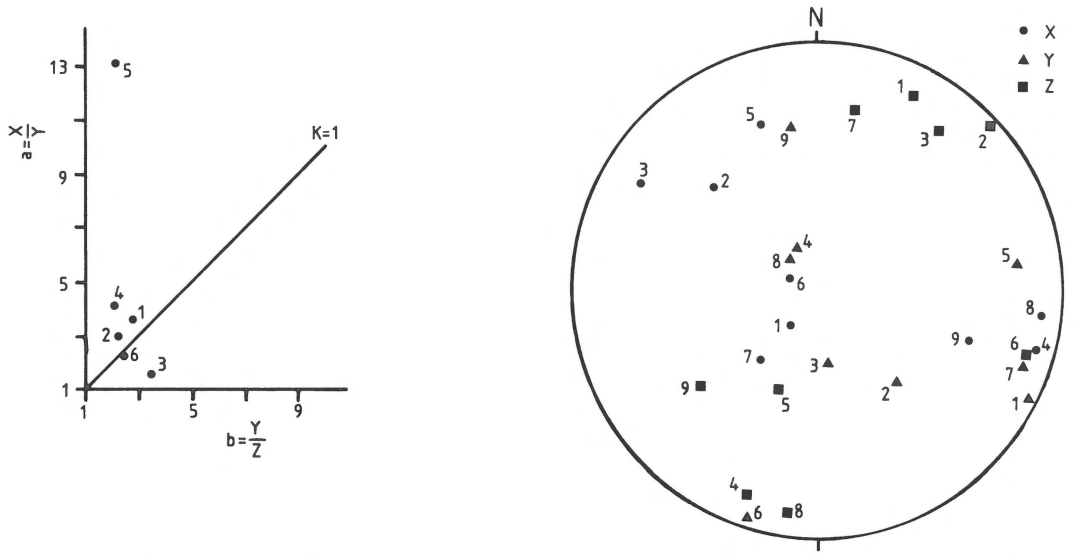

Fig. 5. A) Flinn strain diagram showing shapes of finite strain ellipsoids of deformed agglomerates and xenoliths. Coordinates of locations are: 1 = 6720.70–2483.30; 2 = 6722.40–2492.70; 3 = 6722.55–2493.50; 4 = 6733.70–2468.65; 5 = 6733.70–2464.90; 6 = 6731.70–2481.20. B) Principal strain axis orientations displayed on an equal area, lower hemisphere net. Numbers as in A).

servations of the intracrystalline defect structures of cordierite yield <a> and <c>-dislocations, undulatory extinction, subgrains and minor twinning (Van Roermund & Konert 1990). The cordierite porphyroblasts have grown post-F_1 to syn-F_2.

The garnet gneisses have a well developed foliation (S_1) and a weakly developed crenulation cleavage (S_2). The main mineral paragenesis is quartz, biotite, white mica, plagioclase, K-feldspar, opaque and garnet. The garnet porphyroblasts have grown post-F_1 to syn-F_2.

Cordierite strain ellipsoids

Cordierite porphyroblasts show deformation-induced shapes in handspecimens and optical thinsections (Fig. 4). These shapes point to deformation of single, initially anti-clustered distributed, cordierite porphyroblasts, which is in agreement with optical and electron microscopical observations of the intracrystalline defect structures and deformation mechanisms of cordierite made by Van Roermund & Konert (1990). The deformed cordierite porphyroblasts thus in fact reflect the shape of a strain ellipsoid and provide direct information on F_2 and F_3-strain. The correlation of cordierite shape ellipsoids with the spatial distribution pattern should give identical results about the orientation of axes of strain and the shape of strain ellipsoids. However, the strain intensity as determined by the two methods is not necessarily the same, as the distribution of cordierite correlates with the strain of the matrix, while the shape of the blast reflects the strain of cordierite. These two strains may differ due to differences in competency. This offers a method for a direct shape-distribution correlation. In the Somero area, cordierite porphyroblast ellipses with the largest elongation lie within the S_3 foliation. The direction of elongation is parallel to the mineral lineation.

Results of strain analyses

The states of finite strain of six localities are represented in a Flinn diagram (Flinn 1962). Figure 5a shows that strain ellipsoids are prolate in four, and oblate in two localities. This corresponds to a constrictional and a flattening type of finite strain, respectively (Ramsay 1967). The strain intensity k has been calculated by: k = (a-1)/(b-1), where a = longest axis (X)/intermediate axis (Y) and b = in-

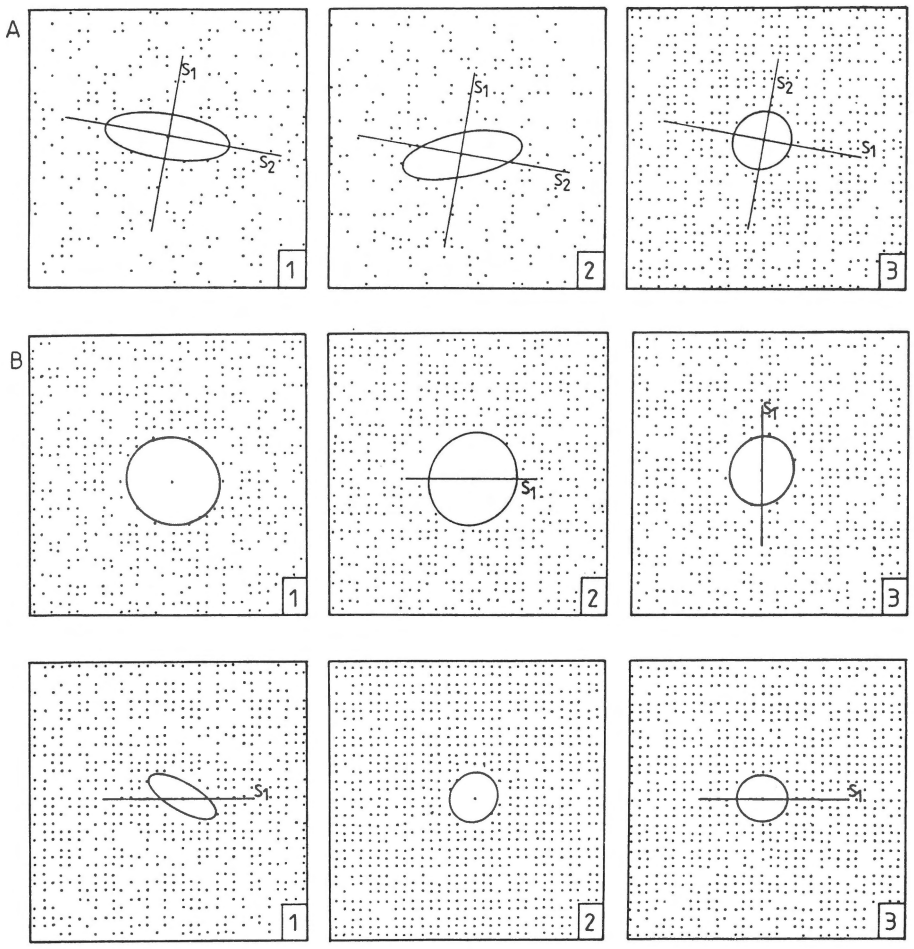

Fig. 6. Plots established by use of the spatial distribution pattern method on cordierite (A) and garnet (B) porphyroblast distributions.
A) Sample RJK 104; sections of sawing are 121/55 (1), 260/36 (2) and 012/73 (3).
B) Sample RJK 88–13; sections of sawing are 153/84 (1), 346/06(2) and 064/89 (3); Sample RJK 88–23; sections of sawing are 110/100 (1), 203/107 (2) and 359/160 (3).

termediate axis (Y)/shortest axis (Z). The finite strain is moderate to high at all localities.

Results of the spatial distribution pattern method, which represent that part of strain after porphyroblast growth, are shown in Fig. 6. Figure 7a illustrates the k-values of the finite strain ellipsoids from the nine localities established. Strain determined by cordierite porphyroblast distributions shows flattening to high constriction (Fig. 7a). The strain values established by garnet porphyroblast distributions indicate plane strain to high constrictional strain.

Correlation of strain data and structure

In the Somero area, two late-tectonic granite domes with a distinct metamorphic evolution and structural style have been recognised (Stel et al. 1989): the Ruostejärvi dome (NE of Somero) and the Halkjärvi dome (SE of Somero) (Fig. 8). The Ruostejärvi dome is a gently westward plunging antiform and shows an increasing grade of metamorphism towards the core. The rocks of this dome have been metamorphosed under low to high amphibolite-facies conditions, where cordierite is the dominant porphyroblast in micaschists and clinopyroxene occurs in metabasites. The cordierite

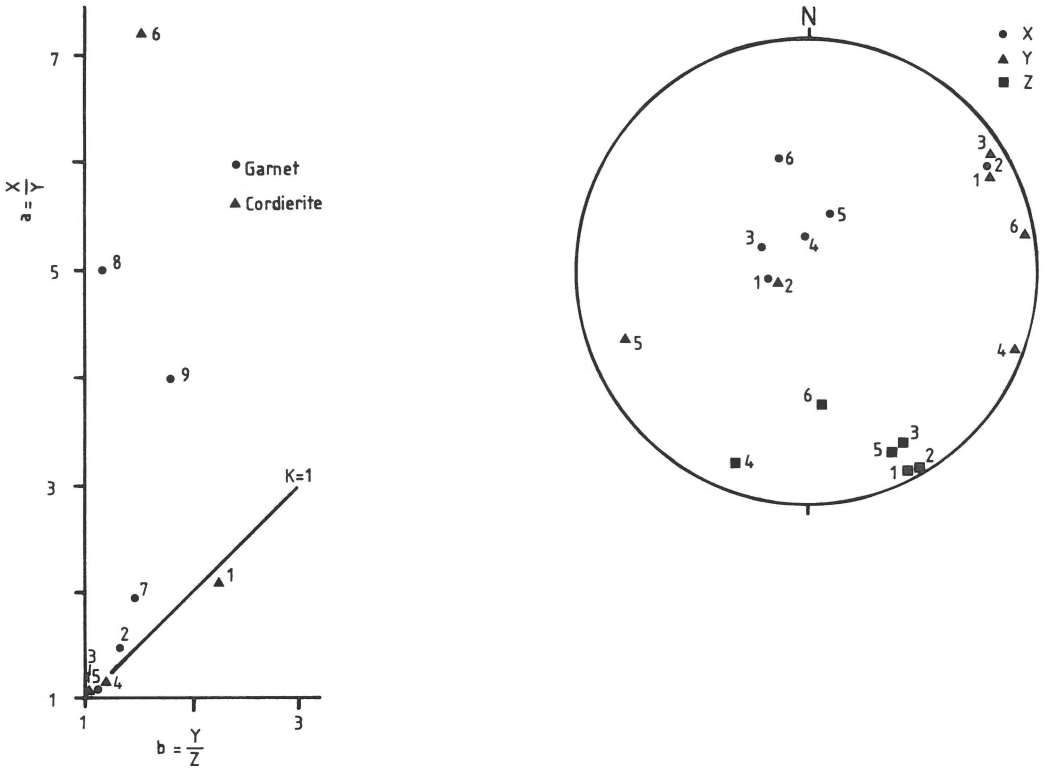

Fig. 7. A) Flinn strain diagram displaying finite strain ellipsoids defined from cordierite and garnet porphyroblast distributions. Samples and locations are: 1 = RJK 104, 6723.60–2481.70; 2 = RJK 88–3, 6732.20–2489.65; 3 = RJK 88–4, 6731.60–2490.50; 4 = RJK 88.8, 6723.70–2480.30; 5 = RJK 88–13, 6710.80–2480.60; 6 = RJK 88–21, 6722.75–2482.90; 7 = RJK 88–23, 6713.10–2488.40; 8 = RJK 88–25, 6711.30–2489.25; 9 = RJK 88–27, 6709.10–2488.90.
B) Principal strain axis orientations presented on an equal area, lower hemisphere projection. Numbers as in A).

porphyroblasts are in contact with K-feldspar and have inclusions of biotite and sillimanite needles, indicating the middle amphibolite-facies conditions reactions of sil + 2bt + qtz + CO_2 = 3crd + Kfs + H_2O (Holdaway & Lee 1977). Leucosomes of migmatites have the character of injection veins emplaced during F_3. The Halkjärvi dome is characterised by (sub)vertical fabric elements and has a high metamorphic grade over the entire structure. The rocks of this dome are almost completely migmatised. Locally cordierite and garnet are in contact, suggesting the granulite-facies metamorphic reaction of crd + bt + qtz = grt + Kfs + V (Winkler 1979). Migmatites are assumed to be the result of in-situ melt generation during F_2. The two domes are separated by the Painio lineament (Fig. 8), of which kinematic indicators (Simpson & Schmid 1983), such as crystallographic fabric asymmetry, composite C-S planar fabrics and asymmetric pressure shadows, illustrate an upward block-movement of the Halkjärvi dome relative to the Ruostejärvi. Using the metamorphic evolution and the sense of movement in the Painio lineament, Stel et al. (1989) propose a deeper erosion level of the Halkjärvi domain in comparison with the Ruostejärvi domain, i.e. an infrastructure and a suprastructure of a granite dome respectively.

There is a close correlation of strain distribution with the large-scale structures in the Somero area. In general, away from the dome structures, the strain values are constrictional, while plane strain to low flattening strain shapes are found close to the mantle-core contact (Figs. 5a, 7a and 8). This is in agreement with a model of interfering (Brun et al. 1981) and ballooning (Bateman 1984) diapirs. Sample RJK 88–21 (Fig. 7a) shows a high strain

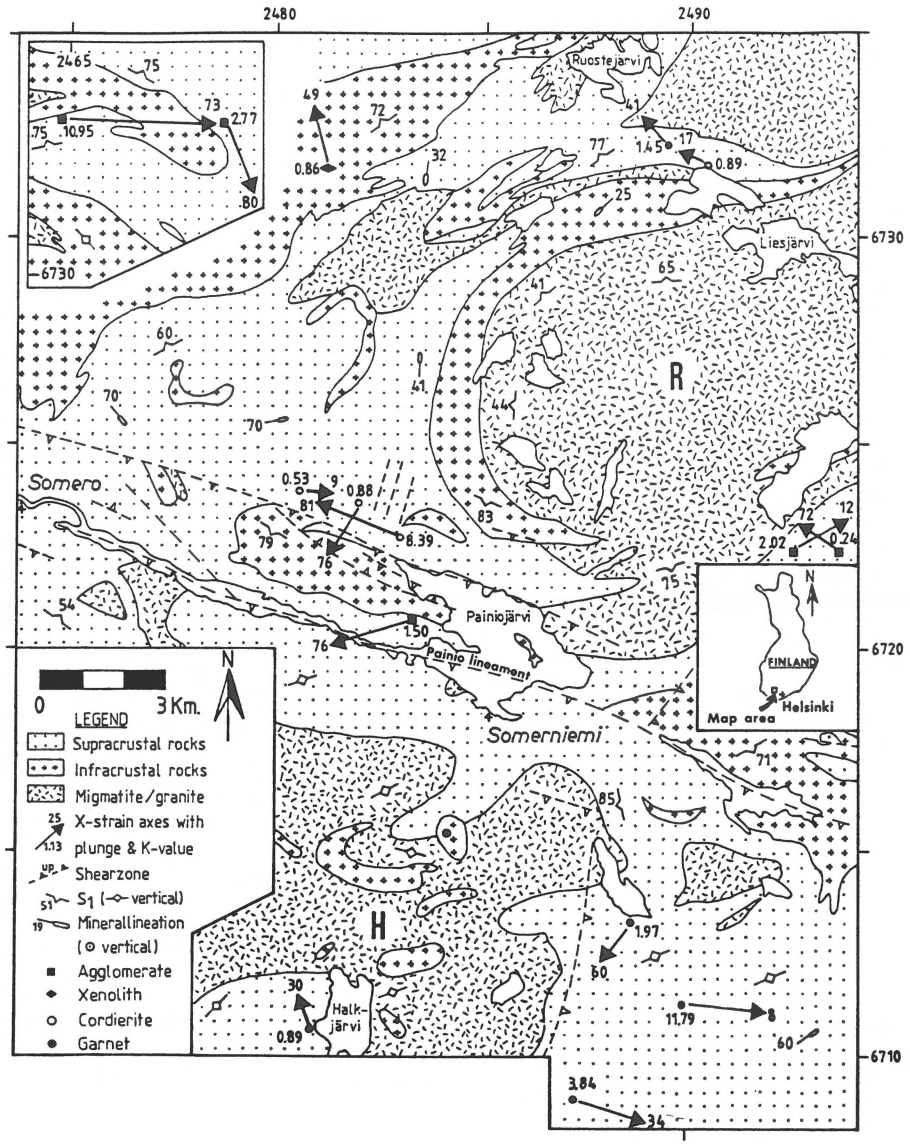

Fig. 8. Simplified geological map of the Somero area with superimposed results of strain analyses performed on agglomerates, xenoliths and cordierite and garnet porphyroblast distributions. R = Ruostejärvi dome and H = Halkjärvi dome.

ratio and has probably been influenced by the NNE-SSW striking shear zone (Fig. 8). Figures 5b and 7b illustrate the orientations of the finite principal ellipsoid axes. The plunge of the longest-axis (X) for agglomerates and xenoliths is moderate to steep, whereas the intermediate (Y) and shortest-axis (Z) have gentle to moderate plunges and azimuths of approximately 060 and 150 respectively (Fig. 5b).

Strain ellipsoids determined from cordierite and garnet porphyroblast distributions, i.e. F_2 and F_3-strain, indicate a gentle plunge of the shortest-axis with a mean azimuth of about 030. When the lengths are almost equal, the orientations of the longest and intermediate-axis are interchangeable and have a mean azimuth of 120, with one steeply plunging and one gently plunging axis (Fig. 7b).

Interpretation

In the Halkjärvi domain, foliations and lineations have a steep to vertical dip and plunge. This domain (infrastructure) is characterised by higher metamorphic conditions than the Ruostejärvi domain (suprastructure). Figure 8 illustrates that finite strain values in the inferred infrastructure are in general larger than those in the suprastructure. In the infrastructural and suprastructural parts it has been observed that the mineral lineation, both inside and outside the bomb-like fragments, and the longest axis of xenoliths coincide with the X-axis of the finite strain ellipsoid. The mineral lineation in the domes is therefore equivalent to a stretching lineation.

There are two scenarios to explain a steep plunge of the X-axis: first, a vertical pre-F_1 tilting of S_o (sedimentary bedding), which involves a nearly vertical extension and thus a practically horizontal shortening as an important deformation; or second, a post-F_1 tilting of foliations and lineations associated with almost horizontal extension. The strain pattern is not conclusive about the timing of vertical tilting of the structural element(s). However, the radial pattern of F_2 and F_3 X-axes of strain associated with the dome structures point to a syngenetic relation (Fig. 8).

Agglomerates and xenoliths have passed through the complete deformational process, thus $F_1 + F_2 + F_3$ strain. However, it is conspicuous that the XY-plane of the finite strain ellipsoid is parallel to S_1 (Figs. 5b and 8). So, the orientation of the finite strain ellipsoid is close to the inferred F_1-related XY plane of strain. This suggests that the values of F_2 and F_3-strain were relatively small in comparison with F_1. Moreover, it was observed that prolate-shaped objects have been folded by F_2 and indicate a constrictional strain during F_1. Constrictional strain during F_1 is in agreement with the strain pattern expected in the infrastructure of a diapir. The finite strain pattern is thus basically the constrictional F_1-strain.

To the north of the Painio lineament, S_2 foliation is microscopically boxfolded with an axial plane striking 290 (Fig. 3) and is parallel to the axial plane of the macroscopial dome (Fig. 8). The axial plane coincides with the XY-plane of the F_3-strain ellipsoid, as determined by cordierite porphyroblasts (Fig. 7b). This indicates a regional horizontal shortening during F_3-diapirism and migmatisation, which however leave no penetrative imprint in the rocks. The syn-F_3 compressional deformation resulted in the squeezing of the domal structures, generating the oval shape and leading locally to the development of F_3-folds. This is in good agreement with Stel et al. (1989) who observed that D_3 refolds earlier structures and proposed F_3-folding to be syngenetic with migmatisation and diapirical processes.

Conclusions

1) The correlation and interpretation of progressive strain data with successive structural elements is possible in the Somero area and yields important information about the structural evolution and the nature of the individual structural elements.
2) Strain analysis based on the spatial distribution of porphyroblasts, such as proposed by Fry (1979), proved to be a useful method to determine strain in the Somero area. The analysis allows the assessment of the strain-history which took place after peak metamorphic conditions.
3) In the Somero area, the shapes of the finite strain ellipsoids, as established on primary markers (agglomerates and xenoliths), resulting from the three superposed ($F_1 + F_2 + F_3$) deformation phases, correlate well with those of F_2 and F_3 ellipsoids, as deduced from porphyroblast distributions.
4) The shape of ellipsoids varies with the structural position relative to the granite domes. Near the granite-country rock interface, oblation strain to plane strain was recorded, while at a distance from this contact zone, constriction strain took place.
5) The good correlation between the finite and ($F_2 + F_3$) strain suggests continuous oblation or constriction along the same axes.
6) The strain pattern is in agreement with a diapir-

ical origin of the granite domes in the Somero area.

Acknowledgements

R. Gras, P. McMahon and G. Shudofsky are kindly thanked for their critical reading of the manuscript. An anonymous reviewer is thanked for suggestions to improve the manuscript.

References

Bateman, R.J. 1984 On the role of diapirism in the segregation, ascent and final emplacement of granitoid magmas – Tectonophysics 110: 211–231

Brun, J.P., D. Gapais & B. Le Theoff 1981 The mantled gneiss domes of Kuopio (Finland): interfering diapirs – Tectonophysics 74: 283–304

Flinn, D. 1962 On folding during three-dimensional progressive deformation – Quart J Geol Soc 118: 385–433

Dietvorst, E.J.L. 1981 Pelitic gneisses from Kemiö, southwest Finland. PhD Thesis, Vrije Universiteit Amsterdam. Rodopi, Amsterdam, 115 pp

Fry, N. 1979 Random point distributions and strain measurement in rocks – Tectonophysics 60: 89–105

Griffin, V.S. Jr. 1979 Diapirism, polydeformation and amoeboidal tectonic patterns in the Svecofennidic area of southwestern Finland. Geol Surv Finland, Rep 41, 16 pp

Hanna, S.S. & N. Fry 1979 A comparison of methods of strain determination in rocks from southwest Dyfed (Pembrokeshire) and adjacent areas – J Struct Geol 1: 155–162

Hietanen, A 1975 Generation of potassium-poor magmas in the northern Sierra Nevada and the Svecofennian in Finland – J Research US Geol Surv 3: 631–645

Holdaway, M.J. & S.M. Lee 1977 Fe-Mg cordierite stability in high-grade pelitic rocks based on experimental, theoretical and natural observations – Contrib Mineral Petrol 63: 175–198

Milton, N.J. 1980 Determination of the strain ellipsoid from measurements on any three sections – Tectonophysics 64: T19–T27

Owens, W.H. 1984 The calculation of a best-fit ellipsoid from elliptical sections on arbitrarily orientated planes – J Struct Geol 6: 571–578

Ramsay, J.G. 1967 Folding and fracturing of rocks. McGraw-Hill, New York, 568 pp

Schreurs, J.M.C.M. 1985 The west Uusimaa low pressure thermal dome, SW Finland. PhD Thesis, Vrije Universiteit Amsterdam. Rodopi, Amsterdam, 179 pp

Simonen, A. 1980 The Precambrian of Finland. Geol Surv Finland, Bull 304, 58 pp

Simpson, C. & S.M. Schmid 1983 An evaluation of criteria to deduce the sense of movement in sheared rocks – Bull Geol Soc America 94: 1281–1288

Spiegel, M.R. 1972 Theory and problems of statistics. McGraw-Hill, New York, 359 pp

Stel, H., R. Veenhof, J.M. Huizenga, M. Timmerman & J.M.H. Hartsink 1989 Infra-supra structure relations of a microcline-granite dome in the Somero area, Svecofennides, SW Finland – Bull Geol Soc Finland 61: 131–141

Van Balen, R.T. & J.D.A.M. Van Wees 1987 Numerieke strainanalyse van gedeformeerde ellips(oide) vormige objecten. Internal report University of Amsterdam

Van Roermund, H.L.M. & R.J. Konert 1990 Deformation and recrystallisation mechanisms in naturally deformed cordierite – Phys Chem Minerals 17: 52–61

Windley, B.F. 1986 The evolving continents. Wiley, New York, 399 pp

Winkler, H.G.F. 1979 Petrogenesis of metamorphic rocks. Springer, New York, 348 pp